

ASSESSMENT OF ION-ATOM COLLISION DATA
FOR MAGNETIC FUSION PLASMA EDGE MODELLING*

R. A. Phaneuf
Controlled Fusion Atomic Data Center
Physics Division
Oak Ridge National Laboratory
Oak Ridge, Tennessee 37831-6372, U.S.A.

CONF-9009283--1
DE91 001920

ABSTRACT

Cross-section data for ion-atom collision processes which play important roles in the edge plasma of magnetically-confined fusion devices are surveyed and reviewed. The species considered include H, He, Li, Be, C, O, Ne, Al, Si, Ar, Ti, Cr, Fe, Ni, Cu, Mo, W and their ions. The most important ion-atom collision processes occurring in the edge plasma are charge-exchange reactions. Excitation and ionization processes are also considered. The scope is limited to atomic species and to collision velocities corresponding to plasma ion temperatures in the 2-200 eV range. Sources of evaluated or recommended data are presented where possible, and deficiencies in the data base are indicated.

FOREWORD

This paper is dedicated to the memory of Clarence F. Barnett, founder of the ORNL Controlled Fusion Atomic Data Center. "Barney" devoted his professional career to the promotion of effective communication between the atomic and fusion research communities, and was still actively engaged in this mission at the time of his death in 1989. The data compilation upon which he was working, entitled "Collisions of H, H₂, He and Li Atoms and Ions with Atoms and Molecules," was published in August, 1990 as part of the Atomic Data for Fusion series, popularly known as "the Redbooks." This compilation is a primary source for much of the data assessment presented in this paper. Barney's critical insights, guidance and dedication will be sorely missed by the data center and by the fusion research community.

I. INTRODUCTION

The edge plasma of magnetically-confined fusion plasmas has received considerable attention [1] due to its pivotal role in insulating the high-temperature core plasma from the vacuum vessel. This interest has been intensified by mounting evidence that the quality of confinement of the hot plasma core depends critically on subtle details of the management of the edge or scrape-off plasma [2].

*Summary of presentation to the Meeting of the IAEA Co-ordinated Research Programme on "Atomic and Molecular Data for Fusion Edge Plasmas," Vienna, Austria, September 24-26, 1990.

"The submitted manuscript has been authored by a contractor of the U.S. Government under contract DE-AC05-84OR21400. Accordingly, the U.S. Government retains a nonexclusive, royalty-free license to publish or reproduce the published form of this contribution, or allow others to do so, for U.S. Government purposes."

DISCLAIMER

This report was prepared as an account of work sponsored by an agency of the United States Government. Neither the United States Government nor any agency thereof, nor any of their employees, makes any warranty, express or implied, or assumes any legal liability or responsibility for the accuracy, completeness, or usefulness of any information, apparatus, product, or process disclosed, or represents that its use would not infringe privately owned rights. Reference herein to any specific commercial product, process, or service by trade name, trademark, manufacturer, or otherwise does not necessarily constitute or imply its endorsement, recommendation, or favoring by the United States Government or any agency thereof. The views and opinions of authors expressed herein do not necessarily state or reflect those of the United States Government or any agency thereof.

Material surfaces (vessel walls, limiters and divertor plates) are the primary sources of neutral particles emanating or recycling into the plasma [3]. Thus atomic processes involving neutral hydrogen, helium (in ignited D-T plasmas), carbon, oxygen and metallic impurities play an important role in the particle, energy and ionization balance in the edge plasma. This region is characterized in general by relatively low ion and electron temperatures (2-200 eV) and moderate to high particle densities (10^{12} - 10^{15} cm⁻³). Molecules and molecular ions also play a role [1], but collisions involving them are excluded from the present discussion; these are addressed specifically in accompanying articles.

Initial surveys of the relative importance of the various atomic reactions occurring in the edge plasma were performed by Janev and co-workers. [4,5] More recent assessments of atomic and molecular data requirements and the available database for modelling and diagnostics of the edge plasma have been made by Tawara and Phaneuf [6], and by Janev et al. [7].

Although electron-impact processes are by far the most frequent and dominant in the edge plasma, heavy-particle collisions (particularly charge-exchange reactions) may also have a significant effect on particle transport and cooling. [1,7] While the atomic data base for reactions which occur in the hotter core plasma or in energetic neutral-beam heating has grown substantially in recent years [8], relatively less attention has been given to such processes at the lower collision energies which prevail in the edge region. This is due to the difficulty in reliably extending experimental measurements for heavy-particle collisions down to eV energies, and also, from a theoretical standpoint, to the need for elaborate quantum-chemical approaches to address such collisions with a degree of confidence.

II. SCOPE OF THIS SURVEY

In this report, available cross-section data for a number of ion-atom collision processes which are important to both the modelling and diagnostics of the edge plasma will be surveyed and reviewed. In the relevant velocity range, the most important processes involve charge exchange, association, electron detachment, and, to a lesser degree, impact excitation. The species considered include H, He, Li, Be, C, O, Ne, Al, Si, Ar, Ti, Cr, Fe, Ni, Cu, Mo, W and their ions [7]. Atoms and ions of hydrogen isotopes are considered to be the primary plasma constituents, as are those of He, which will constitute the ash of ignited D-T plasmas, and will be abundant in the edge plasma. All other species are classified as impurities, for which the maximum charge state considered is +10. Ne, Ar and Li are included because they are frequently introduced for plasma diagnostic purposes.

The reaction rate, the product of the concentrations of the two reactants and the rate coefficient for the process of interest has been chosen to serve as a rough measure of the relative importance

of a given reaction and pair of reactants. The reaction rate for a specific reaction represents the total number of such reactions which take place per unit volume per unit time in the plasma. Thus, in general, reactions involving two primary plasma constituents will be more important than reactions involving one primary and one impurity species, which will, in turn be more important than those involving two impurities. Of course, other factors may also mitigate the relative importance of one reaction compared to another - for example, its effect on the ionization balance, cooling, transport of particles or specific diagnostic measurements. The concentrations of different species may also vary significantly in different plasma devices, or in different operating regimes in the same device.

During the past 5-10 years, considerable effort has been devoted on an international scale to the compilation, assessment and recommendation of atomic-collision data for fusion-relevant processes. Of particular significance to the present survey are reports from the Princeton group [4,5], the Nagoya Data Center [9-12], the JAERI Data Center [12-16], the ORNL Controlled Fusion Atomic Data Center [17-21], the JILA Information Center [22], and Ruhr University [23]. The IAEA Atomic and Molecular Data Unit has co-ordinated a recent assessment of the carbon and oxygen collision database for fusion applications [24]. A number of the reactions covered in the present survey are included in a recently published volume of recommended data by C.F. Barnett [18].

III. GENERAL CONSIDERATIONS FOR HEAVY-PARTICLE COLLISIONS

Because electrons have a much higher velocity than heavy particles at the same temperature, electron collisions with heavy particles occur much more frequently than collisions between heavy particles. Thus, to be of comparable importance, a particular collision process between heavy particles must have a larger cross section to compensate for the reduced collision frequency. Because of the low temperature and relatively short residence time of ions in the edge region, the lower ionization stages are predominant. Therefore, collisions of atoms and impurity ions in the lower ionization stages play a significant role in the dynamics of the edge plasma.

Inelastic processes may be generally classified as to whether they are endoergic, resonant or exoergic. Endoergic processes have a finite threshold energy, usually of the order of several to several tens of eV for the species present in the edge. For such processes, the cross section decreases with decreasing energy, becoming exponentially small at the lowest energies. Resonant or exoergic processes, on the other hand, are characterized by cross sections which often increase with decreasing energy, and these may play an important role at the lower temperatures prevailing in the edge plasma.

Figure 1, taken from a report by Tawara and collaborators [5], compares cross sections for production of various excited states of H by both charge exchange and proton-impact excitation, as

well as that for proton-impact ionization of H. This figure serves to emphasize both the typical availability of data for different processes, and the behavior of the corresponding cross sections for the $H^+ + H$ collision system. While data are not available for processes other than total electron capture at collision energies below 1 keV/amu, it is apparent that these reactions all will have cross sections which are many orders of magnitude smaller than that for total capture in the low-energy region appropriate to the edge plasma. It should be noted that at these energies, electron capture goes almost exclusively into the 1s ground state (i.e., the total cross section at low energies is the same as that for resonant capture into the 1s state).

IV. CHARGE-EXCHANGE COLLISIONS.

Because of the relatively large density of neutral particles, charge-exchange (electron-capture) reactions are by far the dominant inelastic collision processes between heavy particles in the edge plasma. Such reactions generally proceed via avoided crossings of potential-energy curves, and only those which are either resonant or exoergic have appreciable cross sections at energies corresponding to the edge temperature range (2-200 eV). Such temperatures are nonetheless still sufficiently high to produce appreciable impurity ion concentrations in relatively high charge states. Ionization stages up to He-like will be strongly populated for C and O impurities in the edge, and heavier impurities such as Fe and Ni will have appreciable populations in charge states as high as 10.

Of particular importance are symmetric charge-exchange reactions, which are exactly resonant, and charge-exchange reactions involving multiply ionized plasma impurities. The latter are generally exoergic by several to several tens of eV, populating excited levels of the once-less-charged product ion, with relatively large cross sections ($>10^{-15}$ cm²) at low energies. These excited products decay radiatively, cooling the plasma and providing useful diagnostic information.

Table 1 presents a survey of the available total charge-exchange cross-section data at three different relative collision energies characteristic of the edge plasma (2, 20 and 200 eV/amu), along with estimated uncertainties. Evaluated data are included whenever available, as indicated. References are given to the latest available source of evaluated or compiled data, and the reader is referred to those publications for references to the original research articles. In a few cases where newer data have become available, a reference to the specific source is given. The lack of an entry for a reaction at a given energy signifies a lack of data, or a serious inconsistency in the available data. In some cases, the data were extrapolated over a small fraction of their energy range where the energy dependence was weak or clearly suggested, or an interpolation was made between sets of data in different energy ranges. These values are given in parentheses. The accuracies listed in Table 1 are based on a judgment of the overall quality and consistency of the available data, and of

the methods employed to obtain them. Cross-section data are available at higher energies for many relevant reactions which are not included in Table 1. For such data, the reader is referred to the more extensive data compilations [5,9-25].

The selection of specific reactant combinations for inclusion in Table 1 is based on a consideration of the relative abundances of the elements in a typical plasma, as discussed in Section II. Hydrogen (H, D and T) and helium (in an ignited D-T plasma) atoms and ions are considered primary plasma constituents; ions and atoms of all other elements are considered to be secondary constituents (impurities), with correspondingly lower particle densities in the edge. The most important reactions included are those involving two primary constituents (H and He atoms or ions). The next level of importance includes reactions involving a primary and an impurity constituent. Reactions involving two impurity constituents have been excluded from Table 1. For all the ion-atom reactions considered in this report, collisions involving isotopes H, D or T may be assumed to have identical cross sections at the same relative velocity (i.e., same energy in eV/amu). Isotopic effects are expected to be significant only at much lower collision energies.

Evaluated total cross-section data are available for C and O ions colliding with hydrogen and helium atoms [17,20], and for a number of reactions involving H and He and Li atoms and ions [5,18]. Total cross sections for electron capture by heavier impurities (such as partially-stripped Fe ions) from H and He have been measured over a wide energy range, and estimates have been made of the cross sections at low energies using analytical scaling formulae based on theoretical considerations [19]. These have been shown to be reliable for $\text{Fe}^{q+} + \text{H}$ collisions to within 20-25% for charge states $q > 4$, and estimated to be within 50-80% for $\text{Fe}^{q+} + \text{He}$ collisions. These same formulae (and cross-section values in Table 1) may be used for collisions of other heavy ions with H and He with an estimated accuracy of 50-80% [19].

Charge-exchange collisions of impurities with metastable H and He are expected from theoretical considerations to have significantly larger cross sections than those for ground-state atoms, and to populate more highly excited states [25,26]. Although such processes are important for spectroscopic diagnostics [26], almost no data is available at the low energies relevant to the edge plasma.

Table 2 contains cross-section data for electron capture into specific quantum states. The criteria for selection of reactions are the same as those for Table 1. The data for collisions involving H^+ , He^+ and He^{2+} are taken primarily from the recent compilation of Barnett [18]. While such state-selective data are available for a large number of important reactions, very few cross-section measurements or calculations extend down to the lower energies relevant to the edge plasma. In fact, many of the tabulated cross sections are based on extrapolations of the available data, and have correspondingly large uncertainties.

In contrast, partial cross sections for populating specific excited product states are available for many charge exchange reactions involving C^{9+} and O^{9+} ions [10], although for most reactions, only theoretical data are available at energies below 1 keV/amu. Some significant discrepancies exist between the different coupled-states calculations, especially for the non-dominant reaction channels, where the choice of an atomic or molecular basis set has a significant effect on the predicted cross section. The accuracies listed in Table 2 reflect such discrepancies, and also the level of consistency with experimental data, where available (usually at somewhat higher energies). The latter are based on both optical and translational energy spectroscopic techniques. Experimental and theoretical data were reviewed in 1985 by Janev and Winter [25], and data for C^{9+} and O^{9+} colliding with H, H_2 and He were compiled in 1987 by Tawara [10]. More recent results are contained in the topical report on carbon and oxygen collision data [24]. Extensive compilations of both total and state-selective charge exchange cross-section data for collisions of all atoms and ions with helium have recently been published by Wu and collaborators [27]. The state-selective data for $Ar^{9+} + He$ have been taken from this compilation; the data for $Ne^{9+} + H$ and $Ar^{9+} + H$ collisions have been taken directly from the literature.

V. EXCITATION AND IONIZATION COLLISIONS

Ion-impact excitation and ionization are endothermic processes, and little data is available for these reactions at the collision energies relevant to the plasma edge. However, the corresponding cross sections also decrease rapidly with decreasing collision energy below several keV/amu, and become negligibly small at edge-relevant energies. Cross sections for electron-impact excitation, on the other hand, tend to be largest at electron energies in the 10-100 eV region. Thus direct electronic excitation occurs predominantly by electron-impact in the edge plasma [1,7].

Evaluated data for a number of impact excitation reactions involving hydrogen, helium and lithium atoms and ions are included in the recent compilation of Barnett [18]. However, only a small fraction of the ion-atom excitation cross sections extend to collision energies below 1 keV/amu. These are summarized in Table 3, in which most of the cross section values presented result from some extrapolation of the existing data, and therefore have large uncertainties. As noted above, these cross sections are in general relatively small ($<10^{-18}$ cm²) at these low energies. Janev and collaborators [4] have systematically applied analytical scaling formulae based on theoretical considerations in order to estimate cross sections and rate coefficients at the lowest energies for a large number of reactions occurring in hydrogen-helium plasmas. These have included in Table 3 when they are consistent with the evaluated data at higher energies. No reliable data were found for

ionization by heavy-particle impact at energies relevant to the edge plasma, except for detachment from negative ions, which is considered in Section VI.

VI. DETACHMENT AND ASSOCIATION COLLISIONS

The presence and role of negative ions in the plasma edge has yet to be determined. Collisional electron detachment from negative ions is an endoergic process, but the binding energies (electron affinities) are often sufficiently small that cross sections are still appreciable (and measurable) at edge-plasma-relevant collision energies. Associative detachment collisions of negative ions with neutral atoms are characterized by large cross sections which may increase with decreasing collision energy. Data for these two processes are collected in Table 4.

VII. SUMMARY

It is clear from the present survey and analysis that charge-exchange reactions are by far the dominant ion-atom collision processes in the plasma edge. While some experimental and/or theoretical data are available for most important charge-exchange reactions between primary plasma constituents (H and He atoms and ions), only in a relatively few cases do these data extend to the lower energies relevant to the plasma edge. Thus much of the needed data must be estimated by extrapolation or use of scaling formulae, and thus has large uncertainties.

The relevant data base for charge-exchange collisions involving C and O impurity ions is more complete, due to a strong research emphasis on collisions of highly charged ions during the past decade. Total cross-section data are available for almost all reactions, and state-selective data for some, at least at the higher energies prevailing in the edge region. Total and state-selective electron capture cross-section data are also available for most reactions of Ne^{9+} and Ar^{9+} ions with H and He, although usually not at the lower edge-relevant energies. Estimates of total electron-capture cross sections for heavier impurity ions such as iron are available from scaling formulae, but are reliable only for charge states $q > 4$. State-selective data for such processes is virtually non-existent at edge-relevant energies.

Data for direct excitation in ion-atom collisions is extremely sparse at edge-relevant energies, and is virtually non-existent for ionization. These processes are, however, of lesser importance in the edge, because the cross sections become extremely small ($< 10^{-18} \text{ cm}^2$) at such low energies. Some data is available for electron detachment from negative ions, which may have an appreciable cross section at low energies. The presence and role of negative ions in the plasma edge has yet to be ascertained.

ACKNOWLEDGMENTS

The author is grateful to Dr. R. K. Janev and to participants of the IAEA Specialists' Meeting on Review of the Status of Atomic and Molecular Data for Fusion Edge Plasma Studies, September 1989, for valuable discussions which motivated the present survey. The author is also indebted to many colleagues for preparing the comprehensive data compilations which served as convenient sources of much of the data presented in this survey. This work was sponsored by the Office of Fusion Energy of the U.S Department of Energy under Contract No. DE-AC05-84OR21400 with Martin Marietta Energy Systems, Inc.

REFERENCES

1. M.F.A. Harrison, "Atomic and Molecular Collisions in the Plasma Boundary," pp 281-349 in **Physics of Plasma-Wall Interactions in Controlled Fusion**, D. E. Post and R. Behrisch, eds., Plenum (1986).
2. D. H. Crandall, "What's Happening at the Edge of Tokamaks," *Nucl. Instrum. Methods Phys. Res. B27* (1987) 475-485.
3. D. M. Heifetz, "Neutral Particle Transport," pp.695-771 in **Physics of Plasma-Wall Interactions in Controlled Fusion**, D. E. Post and R. Behrisch, eds., Plenum (1986).
4. R. K. Janev, D. E. Post, W. D. Langer, K. Evans, D. B. Heifetz and J. C. Weisheit, "Survey of Atomic Processes in Edge Plasmas," *J. Nucl. Materials* 121 (1984) 10-16.
5. R. K. Janev, W. D. Langer, K. Evans, Jr., and D. E. Post, Jr., "Elementary Processes in Hydrogen-Helium Plasmas," Springer Series on Atoms + Plasmas, Volume 4, Springer-Verlag, Heidelberg (1987).
6. H. Tawara and R. A. Phaneuf, "Atomic and Molecular Data requirements for Fusion Plasma Edge Studies," *Comments At. Mol. Phys.* 21 (1988) 177-193.
7. R. K. Janev, M.F.A. Harrison and H. W. Drawin, "Atomic and Molecular Database for Fusion Plasma Edge Studies," *Nucl. Fusion* 29 (1989) 109-127.
8. R. K. Janev and K. Katsonis, "Recent Progress in the Production and Evaluation of Atomic Data for Fusion," *Nucl. Fusion* 27 (1987) 1493-1546.
9. H. Tawara, Y. Itikawa, Y. Itoh, T. Kato, H. Nishimura, S. Ohtani, H. Takagi, K. Takayanagi and M. Yoshino, "Atomic Data Involving Hydrogens Relevant to Edge Plasmas," Institute of Plasma Physics, Nagoya University Report IPPJ-AM-46 (1986).
10. H. Tawara, "Total and Partial Cross Sections for Electron Capture for C^{q+} ($q=6-2$) and O^{q+} ($q=8-2$) Ions in Collisions with H, H_2 and He Atoms," Institute of Plasma Physics, Nagoya University Report IPPJ-AM-56 (1987).

11. H. Tawara, T Kato and Y. Nakai, "Cross Sections for Charge Transfers of Highly Ionized Ions in Hydrogen Atoms," Institute of Plasma Physics, Nagoya University Report IPPJ-AM-30 (1983).
12. H. Tawara, T. Kato and Y. Nakai, "Cross Sections for Electron Capture and Loss by Positive Ions in Collisions with Atomic and Molecular Hydrogen," *Atomic Data Nucl. Data Tables* 32 (1985) 235-303.
13. Y. Nakai, T. Shirai, T. Tabata and R. Ito, "Cross Sections for Charge Transfer of Hydrogen Atoms and Ions Colliding with Gaseous Atoms and Molecules," *Atomic Data Nucl. Data Tables* 37 (1987) 69-101.
14. Y. Nakai, A. Kikuchi, T. Shirai and M. Sataka, "Data on Collisions of Helium Atoms and Ions with Atoms and Molecules: Cross Sections for Charge Transfer of He^{2+} , He^+ , He and He^- with He , Ne , Ar , Kr and Xe ," Japan Atomic Energy Institute Report JAERI-M 84-069 (1984).
15. Y. Nakai, A. Kikuchi, T. Shirai and M. Sataka, "Data on Collisions of Hydrogen Atoms and Ions with Atoms and Molecules: Cross Sections for Charge Transfer of H , H^+ and H^- with He , Ne , Ar , Kr and Xe ," Japan Atomic Energy Research Institute Report JAERI-M 83-143 (1983).
16. M. Sataka, T. Shirai, A. Kikuchi and Y. Nakai, "Ionization Cross Sections for Ion-Atom and Ion-Molecule Collisions: Ionization Cross Sections for H^+ , H_2^+ , He^+ and He^{++} incident on H , H_2 and He ," Japan Atomic Energy Research Institute Report JAERI-M 9310 (1981).
17. R. A. Phaneuf, R. K. Janev and M. S. Pindzola, "Collisions of Carbon and Oxygen Ions with Electrons, H , H_2 and He ," *Atomic Data for Fusion*, Volume 5, Oak Ridge National Laboratory Report ORNL-6090 (1987)
18. C. F. Barnett, "Collisions of H , H_2 , He and Li Atoms and Ions with Atoms and Molecules," *Atomic Data for Fusion*, Volume 1, Oak Ridge National Laboratory Report ORNL-6086 (1990).
19. R. A. Phaneuf, R. K. Janev and H. T. Hunter, "Charge Exchange Processes Involving Iron Ions," pp. 7-20 in *Recommended Data on Atomic Collision Processes Involving Iron and Its Ions*, Nuclear Fusion Special Supplement (1987).
20. R. K. Janev, R. A. Phaneuf and H. T. Hunter, "Recommended Cross Sections for Electron Capture and Ionization in Collisions of C^{q+} and O^{q+} Ions with H , He and H_2 ," *At. Data Nucl. Data Tables* 40 (1988) 249-281.
21. C. F. Barnett, J. A. Ray, E. Ricci, M. I. Wilker and H. B. Gilbody, "Atomic Data for Controlled Fusion Research," Oak Ridge National Laboratory Report ORNL-5206 (1977).
22. R. K. Janev, J. W. Gallagher and B. H. Bransden, "Evaluated Theoretical Cross-Section Data for Charge Exchange of Multiply Charged Ions with Atoms," JILA Information Center report No. 25, University of Colorado (1984). See also *J. Phys. Chem. Ref. Data* 12 (1983) 829; 12 (1983) 873; 13 (1984) 1199.
23. W. K. Wu, B. A. Huber and K. Wiesemann, "Cross Sections for Electron Capture by Neutral and Charged Particles in Collisions with Helium," *At. Data Nucl. Data Tables* 40 (1988) 57-200; 42 (1989) 157-185.

24. R. K. Janev, ed., "Carbon and Oxygen Collision Data for Fusion Plasma Research," *Physica Scripta T28* (1989) [Proceedings of a Topical Meeting of the IAEA, Vienna, 12-13 May, 1988].
25. R. K. Janev and H. Winter, "State-Selective Electron Capture in Atom-Highly Charged Ion Collisions," *Physics Reports* 117, 265-387 (1985).
26. R. C. Isler and R. E. Olson, *Phys. Rev. A* 37 (1988) 3399.
27. T. Tabata, R. Ito, Y. Nakai, T. Shirai, M. Sataka and T. Suguira, *Nucl. Instrum. Methods Phys. Res. B* 31 (1988) 375-81.
28. H. Martinez, C. Cisneros, J. de Urquijo and I. Alvarez, *Phys. Rev. A* 38 (1988) 5914-16.
29. C. C. Havener, M. S. Huq, H. F. Krause, P. A. Schulz and R. A. Phaneuf, *Phys. Rev. A* 39 (1989) 1725.
30. F. G. Wilkie, R. W. McCullough and H. B. Gilbody, *J. Phys. B* 19 (1986) 239-251.
31. L. Opradolce, L. Benmeuraim, R. McCarroll and R. D. Piacentini, *J. Phys. B* 21 (1988) 503-512
32. C. Harel and H. Jouin, *J. Phys. B* 21 (1988) 859-883.
33. R. Baptist, J.J. Bonnet, M. Bonnefoy, E. Boursey, A. Brenac, M. Chassevent, G. Chauvet, S. Dousson, Y. LeDuff, A. Fleury, M. Gargaud and D. Hitz, *Nucl. Instrum. Methods B* 23 (1987) 123-7.
34. C. Can, T. J. Gray, S. L. Varghese, J. M. Hall and L. N. Tunnell, *Phys. Rev. A* 31 (1985) 72-83.
35. T. G. Heil, S. E. Butler and A. Dalgarno, *Phys. Rev. A* 27 (1983) 2365-83.
36. V. V. Afrosimov, D. F. Barash, A. A. Basalaev, K. O. Lozhkin and M. N. Panov, XV International Conference on the Physics of Electronic and Atomic Collisions, Abstracts of Contributed Papers, Brighton, U.K. (1987) 533.
37. M. Bendahman, S. Bliman, S. Dousson, D. Hitz, R. Gayet, J. Hanssen, C. Harel and A. Salin, *J. Phys. (Paris)* 46 (1985) 561-572.
38. F. W. Meyer, A. M. Howald, C. C. Havener and R. A. Phaneuf, *Phys. Rev. A* 32 (1985) 3310-18.
39. S. M. Wilson, R. W. McCullough and H. B. Gilbody, *J. Phys. B* 21 (1988) 1027-35.
40. J. P. Giese, C. L. Cocke, W. Waggoner, L. N. Tunnell and S. L. Varghese, *Phys. Rev. A* 34 (1986) 3770-81
41. L. F. Errea, L. Mendez and A. Riera, *Z. Phys. D* 14 (1989) 229-236.
42. F. Rahman and B. Hird, *Atomic Data Nucl. Data Tables* 35 (1986) 123-83.

TABLE 1. EDGE PLASMA ION-ATOM TOTAL CHARGE-EXCHANGE CROSS SECTIONS

Reaction	Cross Section (cm ²)*			Status [#]	Accuracy ^{&}	Reference
	E=2 eV/amu	20 eV/amu	200 eV/amu			
H ⁺ + H → H + H ⁺	3.8×10	2.9×10 ⁻¹⁵	2.2×10 ⁻¹⁵	ev	A A A	18
H ⁺ + He → He + H ⁺	X	X	2.5×10 ⁻²⁰	ev	X X C	18
H ⁺ + He → H ⁺ + He ²⁺	X	X	(6×10 ⁻²³)	ev	X X E	18
H ⁺ + Li → H + Li ⁺	X	(3×10 ⁻¹⁸)	1.6×10 ⁻¹⁶	ev	X E C	18,27
H ⁺ + Ne → H + Ne ⁺	X	X	8×10 ⁻²¹	co	X X E	15
H ⁺ + Ar → H + Ar ⁺	X	X	4×10 ⁻¹⁷	co	X X D	15
H ⁻ + H → H + H ⁻	1.3×10 ⁻¹⁴	9.0×10 ⁻¹⁵	4.2×10 ⁻¹⁵	ev	C C C	18
He ⁺ + H → He + H ⁺	X	X	2.5×10 ⁻¹⁷	ev,nd	X X D	18,41
He ⁺ + He → He + He ⁺	2.1×10 ⁻¹⁵	1.5×10 ⁻¹⁵	1.1×10 ⁻¹⁵	ev	B B B	18
He ⁺ + Li → He + Li ⁺	X	X	3.3×10 ⁻¹⁵	ev	X X C	18
He ⁺ + Ne → He + Ne ⁺	X	(5×10 ⁻¹⁸)	8×10 ⁻¹⁷	co,nd	X D C	14,28
He ⁺ + Ar → He + Ar ⁺	X	2×10 ⁻¹⁶	2.5×10 ⁻¹⁶	co	X E E	14
He ²⁺ + H → He ⁺ + H ⁺	X	X	3.1×10 ⁻¹⁸	ev	X X C	18
He ²⁺ + He → He ⁺ + He ⁺	2.2×10 ⁻²⁰	2.2×10 ⁻¹⁹	3.0×10 ⁻¹⁸	ev	B B B	18
He ²⁺ + He → He + He ²⁺	(5×10 ⁻¹⁶)	4.1×10 ⁻¹⁶	3.2×10 ⁻¹⁶	ev	C B B	18
He ²⁺ + Li → He ⁺ + Li ⁺	X	X	7.0×10 ⁻¹⁵	ev	X X C	18
Be ⁴⁺ + H → Be ³⁺ + H ⁺	X	X	2.5×10 ⁻¹⁵	nd	X X C	39,40
Be ⁴⁺ + He → Be ³⁺ + He ⁺	X	X	(2.5×10 ⁻¹⁶)	co	X X D	23
C ⁺ + H → C + H ⁺	X	(5×10 ⁻¹⁷)	1.4×10 ⁻¹⁶	ev	X C B	17,20
C ²⁺ + H → C ⁺ + H ⁺	5.1×10 ⁻¹⁹	3.2×10 ⁻¹⁷	3.7×10 ⁻¹⁶	ev	C B B	17,20
C ²⁺ + He → C ⁺ + He ⁺	5.9×10 ⁻¹⁷	3.5×10 ⁻¹⁶	6.0×10 ⁻¹⁶	ev	C C C	17,20
C ³⁺ + H → C ²⁺ + H ⁺	2.1×10 ⁻¹⁵	1.0×10 ⁻¹⁵	5.2×10 ⁻¹⁶	ev	B B B	17,20
C ³⁺ + He → C ²⁺ + He ⁺	3.2×10 ⁻¹⁶	1.1×10 ⁻¹⁵	1.8×10 ⁻¹⁵	ev	D D D	17,20
C ⁴⁺ + H → C ³⁺ + H ⁺	1.1×10 ⁻¹⁵	1.4×10 ⁻¹⁵	3.0×10 ⁻¹⁵	ev	C B B	17,20
C ⁴⁺ + He → C ³⁺ + He ⁺	X	(8×10 ⁻¹⁸)	4.4×10 ⁻¹⁷	ev	X C C	17,20
C ⁴⁺ + He → C ²⁺ + He ²⁺	X	(4×10 ⁻¹⁷)	3.4×10 ⁻¹⁶	ev	X C B	17,20

*Cross sections in parentheses represent an extrapolation of existing data.

[#]"ev" denotes evaluated data, "co" denotes data compilation, "sc" denotes scaling formula, "nd" indicates newer data available (reference given).

[&]Accuracy: A+ <3% A <10% B 10-25% C 25-50% D 50-100% E >100%

Table 1 (Cont'd.)

Reaction	Cross Section (cm ²)*			Status [#]	Accuracy ^{&}	Reference
	E=2 eV/amu	20 eV/amu	200 eV/amu			
C ⁵⁺ + H - C ⁴⁺ + H ⁺	6.0×10 ⁻¹⁵	3.3×10 ⁻¹⁵	2.1×10 ⁻¹⁵	ev	C C B	17,20
C ⁵⁺ + He - C ⁴⁺ + He ⁺	X	X	(1×10 ⁻¹⁵)	ev	X X C	17,20
C ⁶⁺ + H - C ⁵⁺ + H ⁺	2.4×10 ⁻¹⁸	6.0×10 ⁻¹⁷	1.4×10 ⁻¹⁵	ev	C C B	17,20
C ⁶⁺ + He - C ⁵⁺ + He ⁺	X	X	4.4×10 ⁻¹⁶	ev	X X C	17,20
O ⁺ + H - O + H ⁺	1.5×10 ⁻¹⁵	1.2×10 ⁻¹⁵	9.1×10 ⁻¹⁵	ev	B B B	17,20
O ⁺ + He - O + He ⁺	2.4×10 ⁻¹⁷	3.9×10 ⁻¹⁷	8.0×10 ⁻¹⁷	ev	D D D	17,20
O ²⁺ + H - O ⁺ + H ⁺	8.5×10 ⁻¹⁶	6.4×10 ⁻¹⁶	3.4×10 ⁻¹⁶	ev	D D C	17,20
O ²⁺ + He - O ⁺ + He ⁺	4.6×10 ⁻¹⁶	1.1×10 ⁻¹⁵	1.2×10 ⁻¹⁵	ev	C C C	17,20
O ³⁺ + H - O ²⁺ + H ⁺	6.3×10 ⁻¹⁵	3.7×10 ⁻¹⁵	2.9×10 ⁻¹⁵	ev	C C B	17,20
O ³⁺ + He - O ²⁺ + He ⁺	2.6×10 ⁻¹⁶	1.6×10 ⁻¹⁶	1.6×10 ⁻¹⁶	ev	E E E	17,20
O ⁴⁺ + H - O ³⁺ + H ⁺	1.9×10 ⁻¹⁶	9.6×10 ⁻¹⁶	3.2×10 ⁻¹⁵	ev	C C B	17,20
O ⁴⁺ + He - O ³⁺ + He ⁺	1.8×10 ⁻¹⁶	1.4×10 ⁻¹⁶	3.1×10 ⁻¹⁶	ev	D D D	17,20
O ⁵⁺ + H - O ⁴⁺ + H ⁺	4.0×10 ⁻¹⁵	8.8×10 ⁻¹⁵	4.5×10 ⁻¹⁵	ev,nd	D C B	17,20,28
O ⁵⁺ + He - O ⁴⁺ + He ⁺	X	X	(3×10 ⁻¹⁵)	ev	X X C	17,20
O ⁶⁺ + H - O ⁵⁺ + H ⁺	X	X	3.6×10 ⁻¹⁵	ev	X X B	17,20
O ⁶⁺ + He - O ⁵⁺ + He ⁺	X	X	(9×10 ⁻¹⁶)	ev	X X D	17,20
O ⁷⁺ + H - O ⁶⁺ + H ⁺	X	(5×10 ⁻¹⁵)	5.0×10 ⁻¹⁵	ev	X C B	17,20
O ⁷⁺ + He - O ⁶⁺ + He ⁺	X	X	(9×10 ⁻¹⁶)	ev	X X D	17,20
O ⁸⁺ + H - O ⁷⁺ + H ⁺	X	X	2.0×10 ⁻¹⁵	ev	X X B	17,20
O ⁸⁺ + He - O ⁷⁺ + He ⁺	X	X	(2×10 ⁻¹⁵)	ev	X X D	17,20
Ne ⁺ + He - Ne + He ⁺	X	(5×10 ⁻¹⁹)	(3×10 ⁻¹⁷)	co	X E E	23
Ne ²⁺ + H - Ne ⁺ + H ⁺	X	(2×10 ⁻¹⁷)	5×10 ⁻¹⁷	co,nd	X D D	12,34
Ne ²⁺ + He - Ne ⁺ + He ⁺	4×10 ⁻²⁰	1.4×10 ⁻¹⁷	2.5×10 ⁻¹⁷	co	C B B	23
Ne ²⁺ + He - Ne + He ²⁺	X	X	3.5×10 ⁻¹⁸	co	X X B	23

*Cross sections in parentheses represent an extrapolation of existing data.

[#]"ev" denotes evaluated data, "co" denotes data compilation, "sc" denotes scaling formula, "nd" indicates newer data available (reference given).

[&]Accuracy: A+ <3% A <10% B 10-25% C 25-50% D 50-100% E >100%

Table 1 (Cont'd.)

Reaction	Cross Section (cm ²)*			Status*	Accuracy ^{&}	Reference
	E=2 eV/amu	20 eV/amu	200 eV/amu			
Ne ³⁺ + H → Ne ²⁺ + H ⁺	4×10 ⁻¹⁵	(3×10 ⁻¹⁵)	1.8×10 ⁻¹⁵	co,nd	D D C	12,34,35,36,39
Ne ³⁺ + He → Ne ²⁺ + He ⁺	X	(2.2×10 ⁻¹⁶)	1.2×10 ⁻¹⁶	co	X C C	23
Ne ³⁺ + He → Ne ⁺ + He ²⁺	X	X	1.0×10 ⁻¹⁷	co	X X B	23
Ne ⁴⁺ + H → Ne ³⁺ + H ⁺	X	(1×10 ⁻¹⁵)	1.8×10 ⁻¹⁵	co,nd	X D B	12,34,36
Ne ⁴⁺ + He → Ne ³⁺ + He ⁺	X	X	1.7×10 ⁻¹⁵	co	X X B	23
Ne ⁴⁺ + He → Ne ²⁺ + He ²⁺	X	X	8×10 ⁻¹⁷	co	X X C	23
Ne ⁵⁺ + H → Ne ⁴⁺ + H ⁺	X	X	2.5×10 ⁻¹⁵	co,nd	X X C	12,34
Ne ⁵⁺ + He → Ne ⁴⁺ + He ⁺	X	(1×10 ⁻¹⁵)	1.6×10 ⁻¹⁵	co	X C B	23
Ne ⁶⁺ + H → Ne ⁵⁺ + H ⁺	X	X	1.3×10 ⁻¹⁵	nd	X X C	34
Ne ⁶⁺ + He → Ne ⁵⁺ + He ⁺	X	(9×10 ⁻¹⁶)	1.2×10 ⁻¹⁵	co	X C B	23
Ne ⁷⁺ + H → Ne ⁶⁺ + H ⁺	X	X	(3×10 ⁻¹⁵)	nd	X X C	34
Ne ⁷⁺ + He → Ne ⁶⁺ + He ⁺	X	(2×10 ⁻¹⁵)	2×10 ⁻¹⁵	co	X C C	23
Ne ⁸⁺ + H → Ne ⁷⁺ + H ⁺	X	X	(8×10 ⁻¹⁵)	co	X X D	12
Ne ⁸⁺ + He → Ne ⁷⁺ + He ⁺	X	(2×10 ⁻¹⁵)	2×10 ⁻¹⁵	co	X C B	23
Ne ⁹⁺ + H → Ne ⁸⁺ + H ⁺	X	X	7.3×10 ⁻¹⁵	co,nd	X X B	12,38
Ne ¹⁰⁺ + H → Ne ⁹⁺ + H ⁺	X	X	(6×10 ⁻¹⁵)	co,nd	X X C	12,37,38
Al ²⁺ + H → Al ⁺ + H ⁺	X	5×10 ⁻¹⁷	3.5×10 ⁻¹⁶	co	X C C	23
Al ²⁺ + He → Al ⁺ + He ⁺	X	X	2×10 ⁻¹⁶	co	X X E	23
Al ³⁺ + H → Al ²⁺ + H ⁺	X	(1.5×10 ⁻¹⁵)	X	co	X D X	23
Al ³⁺ + He → Al ²⁺ + He ⁺	X	(1×10 ⁻¹⁷)	3×10 ⁻¹⁷	co	X E D	23
Al ³⁺ + He → Al ⁺ + He ²⁺	X	X	(3×10 ⁻¹⁷)	co	X X E	23
Al ⁴⁺ + H → Al ³⁺ + H ⁺	X	(4×10 ⁻¹⁵)	(4×10 ⁻¹⁵)	co	X C C	23
Al ⁴⁺ + He → Al ³⁺ + He ⁺	X	(4×10 ⁻¹⁶)	(2×10 ⁻¹⁵)	co	X E D	23
Al ⁴⁺ + He → Al ²⁺ + He ²⁺	X	X	(4×10 ⁻¹⁶)	co	X X E	23
Al ⁵⁺ + H → Al ⁴⁺ + H ⁺	X	(4×10 ⁻¹⁵)	(4×10 ⁻¹⁵)	co	X C C	23

*Cross sections in parentheses represent an extrapolation of existing data.

*"ev" denotes evaluated data, "co" denotes data compilation, "sc" denotes scaling formula, "nd" indicates newer data available (reference given).

[&]Accuracy: A+ <3% A <10% B 10-25% C 25-50% D 50-100% E >100%

Table 1 (Cont'd.)

Reaction	Cross Section (cm ²)*			Status [#]	Accuracy [‡]	Reference
	E=2 eV/amu	20 eV/amu	200 eV/amu			
Al ⁵⁺ + H → Al ⁴⁺ + H ⁺	X	(4×10 ⁻¹⁵)	(4×10 ⁻¹⁵)	co	X C C	23
Al ⁵⁺ + He → Al ⁴⁺ + He ⁺	X	X	1.2×10 ⁻¹⁵	co	X X B	23
Al ⁵⁺ + He → Al ³⁺ + He ²⁺	X	X	3×10 ⁻¹⁶	co	X X C	23
Al ⁶⁺ + H → Al ⁵⁺ + H ⁺	X	(4×10 ⁻¹⁵)	(4×10 ⁻¹⁵)	co	X C C	23
Al ⁷⁺ + H → Al ⁶⁺ + H ⁺	X	(8×10 ⁻¹⁵)	(8×10 ⁻¹⁵)	co	X C C	23
Al ⁸⁺ + H → Al ⁷⁺ + H ⁺	X	(7×10 ⁻¹⁵)	(7×10 ⁻¹⁵)	co	X C C	23
Al ⁹⁺ + H → Al ⁸⁺ + H ⁺	X	(8×10 ⁻¹⁵)	(8×10 ⁻¹⁵)	co	X C C	23
Al ¹⁰⁺ + H → Al ⁹⁺ + H ⁺	X	(9×10 ⁻¹⁵)	(9×10 ⁻¹⁵)	co	X C C	23
Si ⁴⁺ + He → Si ³⁺ + He ⁺	1.9×10 ⁻¹⁵	1.2×10 ⁻¹⁵	1×10 ⁻¹⁵	co	C C D	23
Ar ⁺ + He → Ar + He ⁺	6×10 ⁻¹⁹	(8×10 ⁻¹⁷)	(2×10 ⁻¹⁶)	co	C E E	23
Ar ²⁺ + H → Ar ⁺ + H ⁺	X	(7×10 ⁻¹⁸)	1.3×10 ⁻¹⁶	co	X D B	12
Ar ²⁺ + He → Ar ⁺ + He ⁺	5×10 ⁻¹⁶	3×10 ⁻¹⁶	4×10 ⁻¹⁶	co	C B B	23
Ar ²⁺ + He → Ar + He ²⁺	X	X	6×10 ⁻¹⁹	co	X X C	23
Ar ³⁺ + H → Ar ²⁺ + H ⁺	X	X	(2.5×10 ⁻¹⁵)	co	X X C	12
Ar ³⁺ + He → Ar ²⁺ + He ⁺	5.5×10 ⁻¹⁷	1.0×10 ⁻¹⁶	5×10 ⁻¹⁶	co	B B C	23
Ar ³⁺ + He → Ar ⁺ + He ²⁺	X	X	3×10 ⁻¹⁸	co	X X C	23
Ar ⁴⁺ + H → Ar ³⁺ + H ⁺	X	(3×10 ⁻¹⁵)	4.0×10 ⁻¹⁵	co	X C B	12
Ar ⁴⁺ + He → Ar ³⁺ + He ⁺	(1×10 ⁻¹⁵)	1.0×10 ⁻¹⁵	8×10 ⁻¹⁶	co	C B B	23
Ar ⁴⁺ + He → Ar ³⁺ + He ²⁺ + e	X	X	(1.2×10 ⁻¹⁷)	co	X X D	23
Ar ⁴⁺ + He → Ar ²⁺ + He ²⁺	X	X	3×10 ⁻¹⁷	co	X X B	23
Ar ⁵⁺ + H → Ar ⁴⁺ + H ⁺	X	X	(4.4×10 ⁻¹⁵)	co	X X C	12
Ar ⁵⁺ + He → Ar ⁴⁺ + He ⁺	X	2.0×10 ⁻¹⁵	1.9×10 ⁻¹⁵	co	X B B	23
Ar ⁵⁺ + He → Ar ⁴⁺ + He ²⁺ + e	X	X	(3×10 ⁻¹⁷)	co	X X D	23
Ar ⁵⁺ + He → Ar ³⁺ + He ²⁺	X	1.4×10 ⁻¹⁶	1.8×10 ⁻¹⁶	co	X C C	23

*Cross sections in parentheses represent an extrapolation of existing data.

[#]"ev" denotes evaluated data, "co" denotes data compilation, "sc" denotes scaling formula, "nd" indicates newer data available (reference given).

[‡]Accuracy: A+ <3% A <10% B 10-25% C 25-50% D 50-100% E >100%

Table 1 (Cont'd.)

Reaction	Cross Section (cm ²)*			Status [#]	Accuracy ^{&}	Reference
	E=2 eV/amu	20 eV/amu	200 eV/amu			
Ar ⁶⁺ + H → Ar ⁵⁺ + H ⁺	X	X	4.5×10 ⁻¹⁵	co	X X B	12
Ar ⁶⁺ + He → Ar ⁵⁺ + He ⁺	X	2.0×10 ⁻¹⁵	2.2×10 ⁻¹⁵	co	X B B	23
Ar ⁶⁺ + He → Ar ⁵⁺ + He ²⁺ + e	X	X	(3.5×10 ⁻¹⁷)	co	X X D	23
Ar ⁶⁺ + He → Ar ⁴⁺ + He ²⁺	X	3.5×10 ⁻¹⁶	8×10 ⁻¹⁶	co	X C C	23
Ar ⁷⁺ + H → Ar ⁶⁺ + H ⁺	X	X	5.3×10 ⁻¹⁵	co	X X B	12
Ar ⁷⁺ + He → Ar ⁶⁺ + He ⁺	X	(2×10 ⁻¹⁵)	2×10 ⁻¹⁵	co	X C B	23
Ar ⁷⁺ + He → Ar ⁶⁺ + He ²⁺ + e	X	X	(4×10 ⁻¹⁷)	co	X X D	23
Ar ⁷⁺ + He → Ar ⁵⁺ + He ²⁺	X	2×10 ⁻¹⁶	5×10 ⁻¹⁶	co	X C C	23
Ar ⁸⁺ + He → Ar ⁷⁺ + He ⁺	X	1.5×10 ⁻¹⁵	1.7×10 ⁻¹⁵	co	X C B	23
Ar ⁸⁺ + He → Ar ⁶⁺ + He ²⁺	X	X	4×10 ⁻¹⁶	co	X X C	23
Ar ⁹⁺ + He → Ar ⁸⁺ + He ⁺	X	X	2.1×10 ⁻¹⁵	co	X X B	23
Ar ⁹⁺ + He → Ar ⁷⁺ + He ²⁺	X	X	8×10 ⁻¹⁷	co	X X C	23
Ar ¹⁰⁺ + He → Ar ⁹⁺ + He ⁺	X	(3×10 ⁻¹⁵)	(3×10 ⁻¹⁵)	co	X C C	23
Ti ²⁺ + H → Ti ⁺ + H ⁺	X	X	3.5×10 ⁻¹⁷	co	X X B	12
Fe ²⁺ + He → Fe ⁺ + He ⁺	X	X	(5×10 ⁻¹⁸)	co	X X C	23
Fe ³⁺ + H → Fe ²⁺ + H ⁺	X	4.4×10 ⁻¹⁵	X	co	X B X	12
Fe ³⁺ + He → Fe ²⁺ + He ⁺	X	X	2×10 ⁻¹⁶	co	E E E	23
Fe ⁴⁺ + H → Fe ³⁺ + H ⁺	X	2.1×10 ⁻¹⁵	X	co	X B X	12
Fe ⁵⁺ + H → Fe ⁴⁺ + H ⁺	4.8×10 ⁻¹⁵	4.8×10 ⁻¹⁵	5.0×10 ⁻¹⁵	co,sc	B B B	12,19
Fe ⁵⁺ + He → Fe ⁴⁺ + He ⁺	2.0×10 ⁻¹⁵	1.7×10 ⁻¹⁵	1.5×10 ⁻¹⁵	sc	D D D	19
Fe ⁶⁺ + H → Fe ⁵⁺ + H ⁺	7.3×10 ⁻¹⁵	5.7×10 ⁻¹⁵	5.7×10 ⁻¹⁵	co,sc	D B C	12,19
Fe ⁶⁺ + He → Fe ⁵⁺ + He ⁺	2.4×10 ⁻¹⁵	2.1×10 ⁻¹⁵	1.8×10 ⁻¹⁵	sc	D D D	19
Fe ⁷⁺ + H → Fe ⁶⁺ + H ⁺	8.6×10 ⁻¹⁵	7.0×10 ⁻¹⁵	6.6×10 ⁻¹⁵	co,sc	D B B	12,19
Fe ⁷⁺ + He → Fe ⁶⁺ + He ⁺	2.8×10 ⁻¹⁵	2.5×10 ⁻¹⁵	2.2×10 ⁻¹⁵	sc	D D D	19

*Cross sections in parentheses represent an extrapolation of existing data.

[#]"ev" denotes evaluated data, "co" denotes data compilation, "sc" denotes scaling formula, "nd" indicates newer data available (reference given).

[&]Accuracy: A+ <3% A <10% B 10-25% C 25-50% D 50-100% E >100%

Table 1 (Cont'd.)

Reaction	Cross Section (cm ²)*			Status [#]	Accuracy ^{&}	Reference
	E=2 eV/amu	20 eV/amu	200 eV/amu			
Fe ⁸⁺ + H → Fe ⁷⁺ + H ⁺	9.8×10 ⁻¹⁵	8.7×10 ⁻¹⁵	7.6×10 ⁻¹⁵	co,sc	D C B	12,19
Fe ⁸⁺ + He → Fe ⁷⁺ + He ⁺	3.2×10 ⁻¹⁵	2.8×10 ⁻¹⁵	2.5×10 ⁻¹⁵	sc	D D D	19
Fe ⁹⁺ + H → Fe ⁸⁺ + H ⁺	1.1×10 ⁻¹⁴	9.8×10 ⁻¹⁵	8.6×10 ⁻¹⁵	co,sc	D C B	12,19
Fe ⁹⁺ + He → Fe ⁸⁺ + He ⁺	3.6×10 ⁻¹⁵	3.2×10 ⁻¹⁵	2.8×10 ⁻¹⁵	sc	D D D	19
Fe ¹⁰⁺ + H → Fe ⁹⁺ + H ⁺	1.2×10 ⁻¹⁴	1.1×10 ⁻¹⁴	9.6×10 ⁻¹⁵	co,sc	D C B	12,19
Fe ¹⁰⁺ + He → Fe ⁹⁺ + He ⁺	4.0×10 ⁻¹⁵	3.5×10 ⁻¹⁵	3.1×10 ⁻¹⁵	sc	D D D	19

*Cross sections in parentheses represent an extrapolation of existing data.

[#]"ev" denotes evaluated data, "co" denotes data compilation, "sc" denotes scaling formula, "nd" indicates newer data available (reference given).

[&]Accuracy: A+ <3% A <10% B 10-25% C 25-50% D 50-100% E >100%

TABLE 2. EDGE PLASMA STATE-SELECTIVE CHARGE-EXCHANGE CROSS SECTIONS

Reaction	Cross Section (cm ²)*			Status [#]	Accuracy ^{&}	Reference
	E=2 eV/amu	20 eV/amu	200 eV/amu			
H ⁺ + H → H(2s) + H ⁺	X	X	(8×10 ⁻²⁰)	ev	X X E	5,18
H ⁺ + H → H(2p) + H ⁺	X	1×10 ⁻¹⁹	3×10 ⁻¹⁸	ev	X E E	5,18
H ⁺ + H(n=2) → H(n=2) + H ⁺	2×10 ⁻¹⁴	1×10 ⁻¹⁴	8×10 ⁻¹⁵	sc	E E E	5
H ⁺ + H(n=3) → H(n=3) + H ⁺	8×10 ⁻¹⁴	6×10 ⁻¹⁴	4×10 ⁻¹⁴	sc	E E E	5
H ⁺ + He → H(2p) + He ⁺	X	X	(1×10 ⁻²¹)	ev	X X E	18
H ⁺ + He → H(3s) + He ⁺	X	X	(4×10 ⁻²⁰)	ev	X X E	18
H ⁺ + He → H(3p) + He ⁺	X	X	(2×10 ⁻²⁰)	ev	X X E	18
H ⁺ + Li → H(2s) + Li ⁺	X	X	(2×10 ⁻¹⁶)	ev	X X E	18
H ⁺ + Li → H(2p) + Li ⁺	X	X	(4×10 ⁻¹⁶)	ev	X X E	18
He ⁺ + H → He(1s2s) + H ⁺	X	X	2.5×10 ⁻¹⁷	nd	X X C	41
He ⁺ + He → He(m) + He ⁺	X	3×10 ⁻¹⁹	3×10 ⁻¹⁸	ev	X C C	18
He ⁺ + He → He(2 ¹ P) + He ⁺	X	X	(1×10 ⁻¹⁸)	ev	X X E	18
He ⁺ + He → He(3 ¹ P) + He ⁺	X	X	(2×10 ⁻¹⁹)	ev	X X E	18
He ⁺ + He → He(3 ³ P) + He ⁺	X	X	2×10 ⁻¹⁹	ev	X X C	18
He ⁺ + He → He(3 ³ D) + He ⁺	X	X	1.3×10 ⁻¹⁸	ev	X X C	18
He ⁺ + He → He(4 ³ S) + He ⁺	X	X	(5×10 ⁻²⁰)	ev	X X E	18
He ⁺ + He → He(4 ³ P) + He ⁺	X	X	3×10 ⁻²⁰	ev	X X C	18
He ⁺ + He → He(4 ³ D) + He ⁺	X	X	2.5×10 ⁻¹⁹	ev	X X C	18
He ²⁺ + H → He ⁺ (2s) + H ⁺	X	(5×10 ⁻²⁴)	5.2×10 ⁻¹⁹	ev	X E E	18
He ²⁺ + H → He ⁺ (2p) + H ⁺	X	X	(1.4×10 ⁻¹⁷)	ev	X X D	18
He ²⁺ + He → He ⁺ (2s) + He ⁺	X	X	(2×10 ⁻¹⁸)	ev	X X E	18
He ²⁺ + Li → He ⁺ (3p) + He ⁺	X	X	(7×10 ⁻¹⁵)	ev	X X C	18,23
He ²⁺ + Li → He ⁺ (4p) + He ⁺	X	X	(1×10 ⁻¹⁶)	ev	X X E	18
C ²⁺ + H → C ⁺ (2s ² 2p ² P) + H ⁺	5×10 ⁻¹⁹	X	X	co	E X X	10
C ²⁺ + H → C ⁺ (2s ² 2p ² D) + H ⁺	3×10 ⁻²⁴	X	X	co	E X X	10
C ³⁺ + H → C ²⁺ (2s3s ³ S) + H ⁺	2×10 ⁻¹⁵	8×10 ⁻¹⁶	3×10 ⁻¹⁶	co,nd	D C B	10,30,31
C ³⁺ + H → C ²⁺ (2p ² 1S) + H ⁺	2×10 ⁻¹⁶	3×10 ⁻¹⁶	1.8×10 ⁻¹⁶	co,nd	D C B	10,31
C ³⁺ + H → C ²⁺ (2s3p) + H ⁺	5×10 ⁻¹⁸	2×10 ⁻¹⁷	3×10 ⁻¹⁷	co,nd	E D C	10,30,31
C ³⁺ + H → C ²⁺ (2s3d) + H ⁺	X	X	3×10 ⁻¹⁷	co,nd	X X C	10,31

*Cross sections in parentheses represent an extrapolation of existing data.

[#]"ev" denotes evaluated data, "co" denotes data compilation, "sc" denotes scaling formula, "nd" indicates newer data available (reference given).

[&]Accuracy: A+ <3% A <10% B 10-25% C 25-50% D 50-100% E >100%

Table 2 (Cont'd.)

Reaction	Cross Section (cm ²)*			Status [#]	Accuracy ^{&}	Reference
	E=2 eV/amu	20 eV/amu	200 eV/amu			
C ⁴⁺ + H → C ³⁺ (3s) + H ⁺	X	X	4×10 ⁻¹⁶	co,nd	X X C	10,32,33
C ⁴⁺ + H → C ³⁺ (3p) + H ⁺	2×10 ⁻¹⁷	9×10 ⁻¹⁶	3×10 ⁻¹⁵	co,nd	E D C	10,32,33
C ⁴⁺ + H → C ³⁺ (3d) + H ⁺	X	5×10 ⁻¹⁶	3×10 ⁻¹⁶	co,nd	X D C	10,32,33
C ⁶⁺ + H → C ⁵⁺ (4s) + H ⁺	X	1×10 ⁻¹⁷	1×10 ⁻¹⁶	co,nd	X D D	10,32
C ⁶⁺ + H → C ⁵⁺ (4p) + H ⁺	X	(4×10 ⁻¹⁷)	3×10 ⁻¹⁶	co,nd	X E D	10,32
C ⁶⁺ + H → C ⁵⁺ (4d) + H ⁺	(1×10 ⁻¹⁸)	3×10 ⁻¹⁷	4×10 ⁻¹⁶	co,nd	E D C	10,32
C ⁶⁺ + H → C ⁵⁺ (4f) + H ⁺	X	3×10 ⁻¹⁷	9×10 ⁻¹⁶	co,nd	X E C	10,32
C ⁶⁺ + He → C ⁵⁺ (3s) + He ⁺	X	X	1.5×10 ⁻¹⁶	co	X X C	10
C ⁶⁺ + He → C ⁵⁺ (3p) + He ⁺	X	X	1×10 ⁻¹⁶	co	X X C	10
C ⁶⁺ + He → C ⁵⁺ (3d) + He ⁺	X	X	3×10 ⁻¹⁶	co	X X E	10
O ²⁺ + H → O ⁺ (2s2p ⁴ P) + H ⁺	8×10 ⁻¹⁶	(8×10 ⁻¹⁶)	X	co	D D X	10
O ²⁺ + He → O ⁺ (2p ³ D) + He ⁺	2×10 ⁻¹⁷	2×10 ⁻¹⁶	3×10 ⁻¹⁶	co	D D D	10,23
O ²⁺ + He → O ⁺ (2p ³ P) + He ⁺	8×10 ⁻¹⁶	1.1×10 ⁻¹⁵	8×10 ⁻¹⁶	co	C C C	10,23
O ³⁺ + H → O ²⁺ (2p3p ³ D) + H ⁺	4×10 ⁻¹⁶	2.5×10 ⁻¹⁶	1.4×10 ⁻¹⁶	co	D D X	10
O ³⁺ + H → O ²⁺ (2p3p ¹ P) + H ⁺	9×10 ⁻¹⁶	9×10 ⁻¹⁶	4×10 ⁻¹⁶	co	C C C	10
O ³⁺ + H → O ²⁺ (2p3p ³ S) + H ⁺	2×10 ⁻¹⁶	2×10 ⁻¹⁶	2×10 ⁻¹⁶	co	E E E	10
O ³⁺ + H → O ²⁺ (2p3s ¹ P) + H ⁺	2×10 ⁻¹⁷	1×10 ⁻¹⁶	2×10 ⁻¹⁶	co	D D D	10
O ³⁺ + H → O ²⁺ (2p3s ³ P) + H ⁺	2×10 ⁻¹⁷	X	X	co	D D D	10
O ⁶⁺ + H → O ⁵⁺ (4s) + H ⁺	X	X	4×10 ⁻¹⁶	co,nd	X X D	10,32
O ⁶⁺ + H → O ⁵⁺ (4p) + H ⁺	X	X	1.7×10 ⁻¹⁶	co,nd	X X D	10,32
O ⁶⁺ + H → O ⁵⁺ (4d) + H ⁺	X	X	9×10 ⁻¹⁶	co,nd	X X E	10,32
O ⁶⁺ + H → O ⁵⁺ (4f) + H ⁺	X	X	1.2×10 ⁻¹⁵	co,nd	X X C	10,32
O ⁶⁺ + He → O ⁵⁺ (3s) + He ⁺	X	X	8×10 ⁻¹⁶	co	X X D	10
O ⁶⁺ + He → O ⁵⁺ (3p) + He ⁺	X	X	2×10 ⁻¹⁶	co	X X E	10
O ⁶⁺ + He → O ⁵⁺ (3d) + He ⁺	X	X	4×10 ⁻¹⁶	co	X X E	10
O ⁸⁺ + H → O ⁷⁺ (5s) + H ⁺	X	X	1.2×10 ⁻¹⁶	co	X X C	10
O ⁸⁺ + H → O ⁷⁺ (5p) + H ⁺	X	X	4×10 ⁻¹⁶	co	X X C	10
O ⁸⁺ + H → O ⁷⁺ (5d) + H ⁺	X	X	4×10 ⁻¹⁶	co	X X C	10
O ⁸⁺ + H → O ⁷⁺ (5f) + H ⁺	X	X	4×10 ⁻¹⁶	co	X X C	10
O ⁸⁺ + H → O ⁷⁺ (5g) + H ⁺	X	X	1×10 ⁻¹⁵	co	X X D	10

*Cross sections in parentheses represent an extrapolation of existing data.

[#]"ev" denotes evaluated data, "co" denotes data compilation, "sc" denotes scaling formula, "nd" indicates newer data available (reference given).

[&]Accuracy: A+ <3% A <10% B 10-25% C 25-50% D 50-100% E >100%

Table 2 (Cont'd.)

Reaction	Cross Section (cm ²)*			Status [#]	Accuracy [‡]	Reference
	E=2 eV/amu	20 eV/amu	200 eV/amu			
Ne ³⁺ + H → Ne ²⁺ (3s) + H ⁺	1×10 ⁻¹⁵	1×10 ⁻¹⁵	2.7×10 ⁻¹⁶	nd	D D B	35,36,39
Ne ³⁺ + H → Ne ²⁺ (3p) + H ⁺	3×10 ⁻¹⁵	2×10 ⁻¹⁵	1.5×10 ⁻¹⁵	nd	D D B	35,36,39
Ne ⁴⁺ + H → Ne ³⁺ (3p) + H ⁺	X	X	2×10 ⁻¹⁶	nd	X X C	36,40
Ne ⁴⁺ + H → Ne ³⁺ (3d) + H ⁺	X	X	1.6×10 ⁻¹⁵	nd	X X C	36,40
Ne ⁵⁺ + H → Ne ⁴⁺ (4s ³ P) + H ⁺	X	X	(5×10 ⁻¹⁶)	nd	X X C	40
Ne ⁵⁺ + H → Ne ⁴⁺ (4s ¹ P) + H ⁺	X	X	(2.0×10 ⁻¹⁵)	nd	X X C	40
Ne ⁶⁺ + H → Ne ⁵⁺ (4s) + H ⁺	X	X	(1.0×10 ⁻¹⁵)	nd	X X C	40
Ne ⁶⁺ + H → Ne ⁵⁺ (4p,4d) + H ⁺	X	X	(3×10 ⁻¹⁶)	nd	X X C	40
Ne ⁷⁺ + H → Ne ⁶⁺ (5s,5p) + H ⁺	X	X	1.6×10 ⁻¹⁵	nd	X X C	40
Ne ⁷⁺ + H → Ne ⁶⁺ (5d) + H ⁺	X	X	1.4×10 ⁻¹⁵	nd	X X C	40
Si ⁴⁺ + He → Si ³⁺ (3s) + He ⁺	8×10 ⁻²⁰	5×10 ⁻¹⁷	6×10 ⁻¹⁶	co	C C C	23
Ar ³⁺ + He → Ar ²⁺ (3p ³ 4s) + He ⁺	X	X	3.5×10 ⁻¹⁶	co	X X C	23
Ar ³⁺ + He → Ar ²⁺ (3p ⁴) + He ⁺	X	X	1×10 ⁻¹⁶	co	X X C	23
Ar ³⁺ + He → Ar ²⁺ (3s3p ⁵) + He ⁺	X	X	5×10 ⁻¹⁷	co	X X C	23
Ar ⁴⁺ + H → Ar ³⁺ (4s) + H ⁺	X	X	3×10 ⁻¹⁶	nd	X X C	36,40
Ar ⁴⁺ + H → Ar ³⁺ (4p) + H ⁺	X	2×10 ⁻¹⁶	3.5×10 ⁻¹⁵	nd	X D C	36,40
Ar ⁴⁺ + H → Ar ³⁺ (3d) + H ⁺	X	X	(1×10 ⁻¹⁶)	nd	X X C	36,40
Ar ⁵⁺ + H → Ar ⁴⁺ (4p) + H ⁺	X	X	4.5×10 ⁻¹⁶	nd	X X C	36,40
Ar ⁵⁺ + H → Ar ⁴⁺ (4d) + H ⁺	X	X	1.6×10 ⁻¹⁵	nd	X X C	36,40
Ar ⁵⁺ + H → Ar ⁴⁺ (4f) + H ⁺	X	X	1.0×10 ⁻¹⁵	nd	X X C	36,40
Ar ⁵⁺ + He → Ar ⁴⁺ (3p4s) + He ⁺	X	X	3×10 ⁻¹⁶	co	X X C	23
Ar ⁶⁺ + H → Ar ⁵⁺ (4f) + H ⁺	X	X	(1.0×10 ⁻¹⁵)	nd	X X C	40
Ar ⁶⁺ + H → Ar ⁵⁺ (5s) + H ⁺	X	X	(1.3×10 ⁻¹⁵)	nd	X X C	40
Ar ⁶⁺ + H → Ar ⁵⁺ (5p) + H ⁺	X	X	(1.9×10 ⁻¹⁵)	nd	X X C	40
Ar ⁶⁺ + H → Ar ⁵⁺ (5d) + H ⁺	X	X	(8×10 ⁻¹⁶)	nd	X X C	40
Ar ⁶⁺ + He → Ar ⁵⁺ (3d) + He ⁺	X	X	2.8×10 ⁻¹⁶	co	X X C	23
Ar ⁶⁺ + He → Ar ⁵⁺ (4s) + He ⁺	X	1×10 ⁻¹⁵	1.1×10 ⁻¹⁵	co	X B B	23

*Cross sections in parentheses represent an extrapolation of existing data.

[#]"ev" denotes evaluated data, "co" denotes data compilation, "sc" denotes scaling formula, "nd" indicates newer data available (reference given).

[‡]Accuracy: A+ <3% A <10% B 10-25% C 25-50% D 50-100% E >100%

Table 2 (Cont'd.)

Reaction		Cross Section (cm ²)*			Status [#]	Accuracy ^{&}	Reference
		E=2 eV/amu	20 eV/amu	200 eV/amu			
Ar ⁶⁺ + He → Ar ⁵⁺ (4p) + He ⁺	X		1.2×10 ⁻¹⁵	1.0×10 ⁻¹⁵	co	X C B	23
Ar ⁷⁺ + H → Ar ⁶⁺ (5p) + H ⁺	X		X	(1.0×10 ⁻¹⁵)	nd	X X C	40
Ar ⁷⁺ + H → Ar ⁶⁺ (5d) + H ⁺	X		X	(3.6×10 ⁻¹⁵)	nd	X X C	40
Ar ⁷⁺ + H → Ar ⁶⁺ (5f) + H ⁺	X		X	(7×10 ⁻¹⁶)	nd	X X C	40
Ar ⁸⁺ + H → Ar ⁷⁺ (5d,5f) + H ⁺	X		X	(5×10 ⁻¹⁶)	nd	X X C	40
Ar ⁸⁺ + H → Ar ⁷⁺ (6s,6p) + H ⁺	X		X	(6×10 ⁻¹⁵)	nd	X X C	40
Ar ⁸⁺ + He → Ar ⁷⁺ (4d) + He ⁺	X		6.4×10 ⁻¹⁶	5.4×10 ⁻¹⁶	co	X C C	23
Ar ⁸⁺ + He → Ar ⁷⁺ (4f) + He ⁺	X		2.3×10 ⁻¹⁵	1.9×10 ⁻¹⁵	co	X C C	23

*Cross sections in parentheses represent an extrapolation of existing data.

[#]"ev" denotes evaluated data, "co" denotes data compilation, "sc" denotes scaling formula, "nd" indicates newer data available (reference given).

[&]Accuracy: A+ <3% A <10% B 10-25% C 25-50% D 50-100% E >100%

TABLE 3. EDGE PLASMA ION-ATOM EXCITATION CROSS SECTIONS

Reaction	Cross Section (cm ²)* E=200 eV/amu	Status*	Accuracy ^{&}	Reference
H ⁺ + He(1 ¹ S) - H ⁺ + He(2 ¹ P)	3×10 ⁻¹⁹	sc	E	5
H ⁺ + Li(2s) - H ⁺ + Li(2p)	(6×10 ⁻¹⁶)	ev	E	18
He ⁺ + H(1s) - He ⁺ + H(2p)	2.2×10 ⁻¹⁷	ev	C	18
He ⁺ + He(1 ¹ S) - He ⁺ + He(3 ³ P)	(2.2×10 ⁻¹⁹)	ev	E	18
He ⁺ + He(1 ¹ S) - He ⁺ + He(3 ³ D)	(1.6×10 ⁻¹⁸)	ev	E	18
He ⁺ + He(1 ¹ S) - He ⁺ + He(4 ¹ S)	(3×10 ⁻²¹)	ev	E	18
He ⁺ + He(1 ¹ S) - He ⁺ + He(4 ¹ D)	(8×10 ⁻²⁰)	ev	E	18
He ⁺ + He(1 ¹ S) - He ⁺ + He(4 ³ P)	(2×10 ⁻²⁰)	ev	E	18
He ⁺ + He(1 ¹ S) - He ⁺ + He(4 ³ D)	(3×10 ⁻¹⁹)	ev	E	18
He ⁺ + Li(2s) - He ⁺ + Li(2p)	(2×10 ⁻¹⁶)	ev	D	18
He ²⁺ + Li(2s) - He ²⁺ + Li(2p)	6.4×10 ⁻¹⁷	sc	E	18

*Cross sections in parentheses represent an extrapolation of existing data.

*"ev" denotes evaluated data, "co" denotes data compilation, "sc" denotes scaling formula, "nd" indicates newer data available (reference given).

[&]Accuracy: A+ <3% A <10% B 10-25% C 25-50% D 50-100% E >100%

TABLE 4. EDGE PLASMA DETACHMENT AND ASSOCIATION CROSS SECTIONS

Reaction	Cross Section (cm ²)*			Status [#]	Accuracy ^{&}	Reference
	E=2 eV/amu	20 eV/amu	200 eV/amu			
H ⁻ + H → H + H + e	4×10 ⁻¹⁶	1.3×10 ⁻¹⁵	1.3×10 ⁻¹⁵	ev	C	5,18
H ⁻ + He → H + He + e	1.3×10 ⁻¹⁶	3.2×10 ⁻¹⁶	4.5×10 ⁻¹⁶	ev	B	18
H ⁻ + H → H ₂ + e	9×10 ⁻¹⁶	5.6×10 ⁻¹⁶	3.8×10 ⁻¹⁶	ev	C	5
He ⁻ + He → He + He + e	X	X	1.3×10 ⁻¹⁵	ev	B	18
Li ⁻ + He → Li + He + e	X	X	4.6×10 ⁻¹⁶	ev	B	18
O ⁻ + He → O + He + e	X	X	5.5×10 ⁻¹⁶	co	B	42

*Cross sections in parentheses represent an extrapolation of existing data.

[#]"ev" denotes evaluated data, "co" denotes data compilation, "sc" denotes scaling formula, "nd" indicates newer data available (reference given).

[&]Accuracy: A+ <3% A <10% B 10-25% C 25-50% D 50-100% E >100%

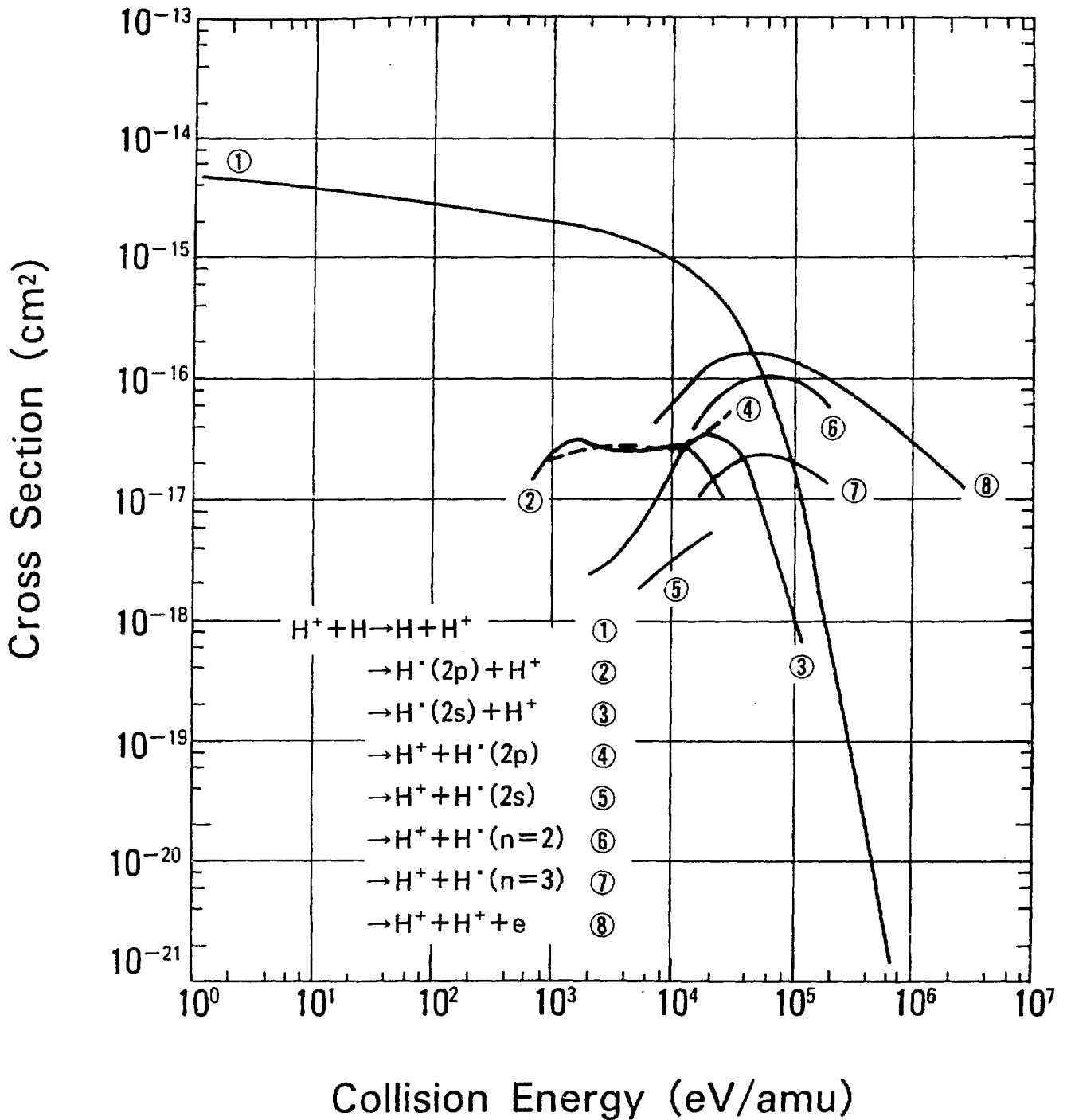


Figure 1. Cross sections for inelastic processes resulting from $H^+ + H$ collisions, taken from the compilation of Tawara et al. [9].